JOURNAL OF RAMAN SPECTROSCOPY
J. Raman Spectrosc. 2007; **38**: 704–713
Published online 8 May 2007 in Wiley InterScience
(www.interscience.wiley.com) DOI: 10.1002/jrs.1731

JRS

Raman scattering from nanomaterials encapsulated into single wall carbon nanotubes

H. Kuzmany,[1] W. Plank,[1] Ch. Schaman,[1] R. Pfeiffer,[1]* F. Hasi,[1] F. Simon,[1,2] G. Rotas,[3] G. Pagona[3] and N. Tagmatarchis[3]

[1] Universität Wien, Institut für Materialphysik, Strudlhofgasse 4, A-1090 Wien, Austria
[2] Budapest University of Technology and Economics, Institute of Physics, H-1521 Budapest P.O. Box 91, Hungary
[3] Theoretical and Physical Chemistry, National Hellenic Research Foundation, 48 Vass. Constantinou Ave., Athens 116, 35, Greece.

Received 28 November 2006; Accepted 25 January 2007

Raman scattering is used to study the filling of single wall carbon nanotubes with C_{60}, $C_{59}N$ and anthracene. It is demonstrated how reversible opening and closing of the tubes can be used to check on the success of the filling process. In the case of $C_{59}N$, filling was performed from the gas phase from 1 : 1 mixture between C_{60} and $C_{59}N$. Comparing the Raman spectra from the encapsulated mixture with the spectra from C_{60} inside the tubes reveals that most of the molecules have reacted to form either the dimer $(C_{59}N)_2$ or the hetero-dimer $C_{60}-C_{59}N$. Anthracene is demonstrated to enter the tubes but the molecule is subjected to a considerable geometrical change including some loss of hydrogens. Copyright © 2007 John Wiley & Sons, Ltd.

KEYWORDS: Raman; nanotubes; fullerenes; $C_{59}N$; anthracene

INTRODUCTION

Among the large variety of nanomaterials known today, single wall carbon nanotubes (SWCNTs) play an exceptional role with respect to Raman scattering. This is on one hand due to the general good response that carbon phases exhibit to Raman spectroscopy and on the other to a strong resonance enhancement of the scattering cross-section for transitions between van Hove singularities in the density of electronic states. The van Hove singularities are a consequence of the one-dimensional nature of the tubes with respect to their electronic structure, as SWCNTs can be understood as rolled-up, very narrow stripes of a single graphene layer.

The other interesting property of the tubes is their hollow core. In contrast to conventional nanowires from, e.g., semiconductors, the tubular character of the SWCNTs provide a nanoscale cavity that can be filled with other materials. Thus the tubes are a well-designed template for the growth of a variety of other nanomaterials. Best known examples are the filling of the tubes with fullerenes,[1] and also inorganic materials such as alkali halides,[2] PbO,[3] HgTe,[4] $FeCl_2$[2] or biological materials such as β-carotene[5] or ice.[6] All these filler compounds exhibit automatically nanodimensions in two directions and are thus candidates for quantum-size effects. In contrast to the transverse direction, they remain macroscopic along the tube axis.

The big advantage of Raman scattering in this field is the possibility to probe the inside of the tubes and study the encapsulated material in its quantized form. In contrast to transmission electron microscopy (TEM) the Raman technique is a bulk method which provides information on the overall character of the tubes and the encapsulated nanomaterial. Alternatively in dedicated experiments, even the response form individual nanotubes can be analyzed.[7]

One general problem in such experiments is picking the right procedure for the filling process, to make sure that the filler material is really deposited inside the tubes and finally to find the percentage of the tubes that are eventually filled.[8] In this paper we therefore discuss at first the possibilities to check that the filler material has really entered the tubes and then apply this method to two special filler materials, namely, the hetero-fullerene $C_{59}N$ and the flat organic molecule, anthracene. The first case is special, since $C_{59}N$ is a magnetic molecule in which the spin of the compound comes from the extra electron on the nitrogen atom. We not only demonstrate the filling process but also the conditions under which the nitrogen spin is retained after the filling. In the second case, we demonstrate filling of the oligo-aromatic structure. In this case the molecule is found to have changed its structure after encapsulation.

*Correspondence to: R. Pfeiffer, Universität Wien, Institut für Materialphysik, Strudlhofgasse 4, A-1090 Wien, Austria.
E-mail: rudolf.pfeiffer@univie.ac.at

RAMAN SCATTERING FROM SWCNTS

SWCNTs are described by two integer numbers n and m which are the components of a lattice vector in the graphene plane. The tube is formed by cutting the graphene plane into a stripe perpendicular to the lattice vector and by a consecutive rolling up of the stripe so that the origin and the tip of the vector coincide. Consequently the resulting diameter of the tubes is given by

$$d = \frac{a}{\pi}\sqrt{m^2 + n^2 + nm} \tag{1}$$

where $a = \sqrt{3}a_{CC}$ is the lattice constant of graphene with the value 0.246 nm and a_{CC} is the carbon–carbon distance in graphene. Appropriate reviews on the structure and properties of carbon nanotubes are given in Refs 9, 10. Tubes with $n = m$ or either m or n equal zero are called armchair or zigzag, respectively, and are achiral. Tubes with $n - m \equiv 0$ (mod 3) are metallic, and all other tubes are semiconducting. This holds at least for a tight binding model. Experimentally, typical tube diameters are 1.4 nm but standard material always exhibits a tube diameter distribution.[11,12] Also, if no particular care is taken, the tubes cluster into bundles of several to several tens individual tubes.

Group theoretical analyses for the Raman active vibrational modes have been reported in several publications.[13,14] According to a very recent review,[15] chiral tubes have 14 Raman active vibrational modes which are distributed into $3A_1 + 5E_1 + 6E_2$ species. For achiral tubes eight Raman active modes can be expected. For zigzag and armchair tubes they are distributed as $2A_{1g} + 3E_{1g} + 3E_{2g}$ and $2A_{1g} + 2E_{1g} + 4E_{2g}$, respectively. Experimentally, only five Raman lines are relevant, but because of the diameter dependence of mode wavenumbers combined with existing diameter distributions in the tube material, the lines can exhibit characteristic splitting. Since resonance Raman spectroscopy is photoselective, this splitting varies with changing laser excitation. Figure 1 depicts the Raman response of the most important lines as excited by three different laser lines. A review of Raman spectra in SWCNTs is provided in Ref. 16.

The lowest wavenumber mode of general importance is the radial breathing mode (RBM). Since this mode depends strongly on the tube diameter, it covers a wavenumber range between 150 and 200 cm^{-1} for standard tubes with mean diameters around 1.4 nm. A most recent reported relation between tube diameter d and RBM wavenumber ν_{RBM} has the form[17]

$$\nu_{RBM} = \frac{C_1}{d} + C_2 \tag{2}$$

with C_1 and C_2 are equal to 222 and 14 cm^{-1}, respectively. Even though this relation is still under discussion and other numbers for C_1 and C_2 have been reported,[18,20,22] it is a convenient relation to discuss the Raman response from SWCNTs. The parameter C_2 describes the tube–tube interaction in SWCNTs bundles or the interaction of the tubes with their environment. For very small diameter tubes, wavenumbers can go beyond 400 cm^{-1}. The observed line pattern depends strongly on the diameter distribution of

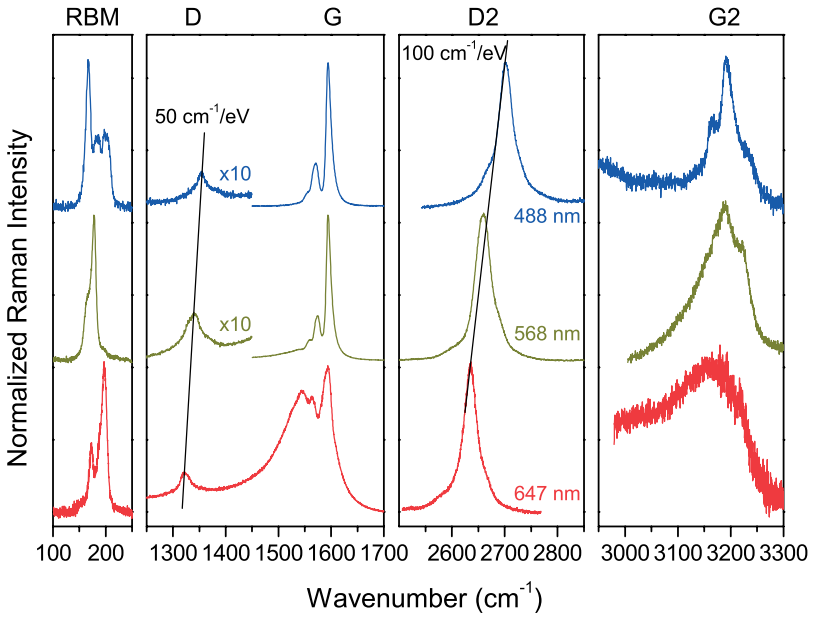

Figure 1. Most important Raman lines of single wall carbon nanotubes as excited with three different laser lines. RBM: radial breathing mode, D: defect-induced line, G: graphitic line, D2: overtone of D-line, G2: overtone of G-line. The thin straight lines indicate the dispersion of the modes. All spectra in one slot were normalized to unit height. This figure is available in colour online at www.interscience.wiley.com/journal/jrs.

the sample and on the exciting laser. In this sense the RBM line is dispersive. The next higher significant feature in the spectra is the D-line, which is defect-induced and originates from a *K*-point phonon. It becomes observable from a double resonance Raman process[23] and exhibits the quasilinear dispersion of the *K*-point phonon. The strong lines around 1590 cm^{-1} (G-lines) are similar to the lines in graphite. However, in contrast to the latter they have six Raman active components.[24] Often only two of them are resolved and assigned as G^+ and G^-. The G-lines exhibit a diameter-dependent wavenumber only for very narrow ($\leq$1 nm) diameter tubes. The remaining two lines are overtones from the D-line (D2 in Fig. 1, at about 2700 cm^{-1}) and from the G-line (G2 in Fig. 1 at about 3200 cm^{-1}. The dispersion of the D2-line is about twice as strong as that of the D-line.

Raman intensities depend critically on the chirality of the tubes. The cross-sections can differ by more than an order of magnitude, even for tubes with very similar diameters.[25] The largest RBM cross-sections were calculated for zigzag and zigzag-like tubes. Interestingly, the intensities for the A_{LO} phonon of semiconducting tubes – the strongest component of the G^+ subband – depend mainly on the tube diameter and only to a very small extent on the tube chirality. With decreasing tube diameters, the Raman cross-section increases in general.[25]

Raman cross-sections have been calculated so far only for band to band transitions. From very recent experimental results[26] and from some detailed calculations,[27] it has become known, however, that almost all oscillator strength for the optical transitions is shifted to the exciton transitions. It is not straightforward that the selective behavior of the cross-sections calculated for band-to-band transitions holds also for the resonance from the exciton transitions. However, it was demonstrated that band-gap transitions and exciton transitions react in the same way to electron–phonon interaction induced changes of transition energies with temperature. Since the Raman cross-sections for both the band gap transitions and the exciton transitions are determined by electron–phonon interaction, exciton resonance cross-sections may behave similarly selective as the band-to-band cross-sections.

EXPERIMENTAL PROCEDURES AND RAMAN CHECK ON THE FILLING

The filling process of SWCNTs consists of two steps. First, the tubes must be opened, which is conveniently done by etching the tubes with oxygen at temperatures around 500 °C under ambient conditions. It is assumed that oxygen first attacks the high curvature areas such as the capped ends. In our case tubes were purchased from Med. Chem. Labs, Moscow. These tubes had already been etched and could therefore be filled as purchased. The nominal tube diameter was 1.4 nm with a Gaussian width (variance) of 0.1 nm. For the filling of the tubes various procedures can be used. The classical way is to heat the tubes together with the filling material in an evacuated sealed quartz tube at a temperature at which the filling material has already a high vapor pressure or even has transformed to the gas phase.[28] This process was applied in our case for the filling with C_{60} and $C_{59}N$ fullerenes. In both cases the filling temperature was 600 °C. The filling time for the $C_{59}N$ molecule was reduced to 15 min to avoid molecule degradation. For this short filling time, about 50% of the maximum filling concentration could be obtained. Filling time for C_{60} was 60 min, as was demonstrated previously. Figure 2 depicts a Raman spectrum of SWCNTs after the filling procedure.

All Raman lines characteristic for the C_{60} fullerene can be observed as sharp features, except the line from $H_g(8)$ which is covered by the G-line from the tubes. The observation that even the highly degenerate H_g Raman lines from the encapsulated C_{60} remain unsplit is surprising. From the non-negligible interaction between the fullerenes and the SWCNTs and the concomitant reduction of the fullerene symmetry, a splitting of the highly degenerate H_g Raman lines could be expected. This splitting is observed only to some extent for the lowest wavenumber H_g mode at 240 cm^{-1}. The strongest line from the fullerenes is the pentagonal pinch mode located at 1466 cm^{-1}. This line is downshifted by 4 cm^{-1} as compared to the same line in the C_{60} crystal at the same temperature. The relative intensity of this line with respect to the G-line from the tubes is a good measure of the success of the filling. According to a previous calibration,[8] an area ratio of 0.32% between the pentagonal pinch mode and the G-line represents 80% filling of the tubes.

The success of the filling process is a critical question in all filling experiments. In cases like fullerenes, high-resolution

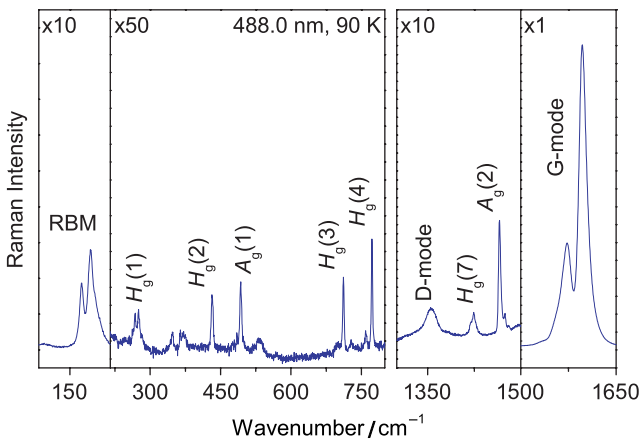

Figure 2. Raman spectrum of SWCNTs after filling with C_{60}. The symbols on the sharp lines assign the modes from the encapsulated fullerenes. The numbers in the top line of the figure give the laser wavelength for excitation, the temperature and scaling factors for the spectrum. This figure is available in colour online at www.interscience.wiley.com/journal/jrs.

DOI: 10.1002/jrs

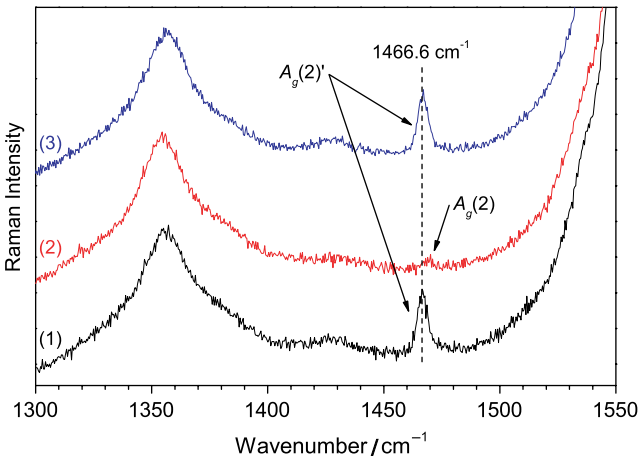

Figure 3. Raman spectra in the spectral range of the pentagonal pinch mode for SWCNTs exposed to C_{60} for filling. (1), (2) and (3) are for tubes with opened ends, after the opened ends were closed by heat treatment and after re-opening the tubes at 500 °C, respectively. Spectra were excited with 488 nm and are normalized to the G-line. The small $A_g(2)$ peak in spectrum (2) is probably due to C_{60} outside the tubes. This figure is available in colour online at www.interscience.wiley.com/journal/jrs.

TEM is a possibility for a qualitative check. However, in other cases enclosed molecules are not easy to see. In particular, special care needs to be applied to prove that the molecules are really inside the tubes and not settled on the outside or in the channels of the tube bundles. Raman spectroscopy offers a possibility to check on this. Line shifts of the inserted molecules are not a safe criterion for a successful filling, since the interaction of the molecules with tubes on the surface of the bundles or in the channels could also lead to line shifts. It turns out that the opened tubes can be re-closed by a heat-treatment at around 800 °C in vacuum. After this treatment the tubes cannot be filled any more. Thus, exposing closed tubes and opened tubes to the same filling process and checking the Raman spectra afterwards provides evidence for a successful filling if the two spectra are characteristically different.[29] Figure 3 gives an example. The broad peak at 1355 cm^{-1} is the D-line of the tubes. The broad structure around 1430 cm^{-1} in spectrum (2) is an unidentified line from the tubes, overlapping in spectra (1) and (3) with the $H_g(7)$ of the fullerene. Interestingly, the closing and opening processes are fully reversible as demonstrated in the figure.

There is even more information available from experiments such as described above. This information can be obtained from a transformation of the filled tubes to double wall carbon nanotubes (DWCNTs) by heat-treatment at 1250 °C.[30] Because of their smaller diameter, the RBMs from the inner tubes appear at much higher wavenumbers, but otherwise, except for some details in the fine structure,[31] follow the diameter distribution from the outer tubes.[32] Figure 4(a) shows some results. In part (a), spectra of DWCNTs are depicted after different pretreatments. Spectrum (1) is obtained after opening the tubes, filling with C_{60} and transformation in the usual way. Tubes represented by spectra (2) and (3) were annealed in vacuum at 1270 and 1000 °C, respectively, after opening and before filling and transformation. Spectrum (4) depicts the result after the annealed tubes were reopened at 500 °C

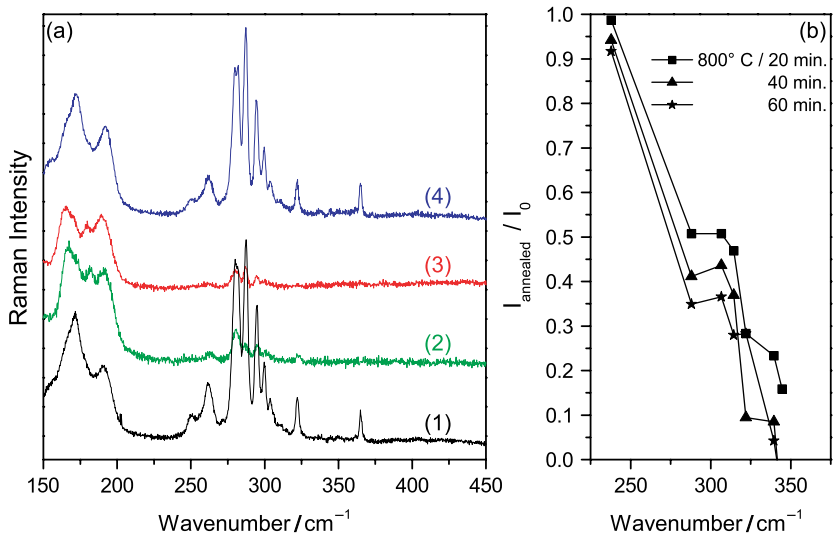

Figure 4. Raman spectra of SWCNTs after different heating and filling procedures and transformation to DWCNTs. (1) for standard filling with C_{60} fullerenes, (2) for annealing at 1270 °C before filling, (3) for annealing at 1000 °C before filling and (4) for re-opening after annealing before filling. Part (b) depicts relative intensities of RBM components from the inner tubes when the outer tubes were partially closed before filling, with respect the same component for a tube that was completely open before filling. This figure is available in colour online at www.interscience.wiley.com/journal/jrs.

before filling. As seen for tubes that were closed before the filling process, the Raman response from the inner tubes is down by more than a factor 10. Part (b) of the figure gives more details. It demonstrates that the closing process is diameter-selective. The tube closing conditions in Fig. 4(b) were 20, 40, and 60 minutes, respectively, at 800 °C.

As an alternative to filling from the gas phase, SWCNTs can also be filled from solutions or from the liquid phase.[33] In the case of anthracene to be discussed below, filling was performed from the liquid phase at a temperature of 500 °C and with an exposure time of 60 min. After the filling process, the anthracene material that remained outside the tube was evaporated at 300 °C.

Raman experiments were performed at 180° back scattering at temperatures between 300 and 80 K with a Dilor xy triple spectrometer in the normal resolution mode. For the excitation of the spectra, various lines from krypton ion, argon ion and He-Ne lasers as well as lines from tunable lasers were used, with a laser power of the order of 1 to about 4 mW. In cases where the Raman line position was critical, the spectrometer was wavenumber-calibrated with gas discharge lamps. This allowed reproducible determination of the wavenumbers of the Raman lines with an accuracy of 1 cm^{-1}, at least for strong lines. For intensity calibration the spectra recorded for the various laser lines were related to the resonance spectrum of Si.

RAMAN RESPONSE FOR TUBES FILLED WITH $C_{59}N$

Owing to the three 2p electrons of nitrogen in the L-shell, the $C_{59}N$ molecule can contribute one extra electron to the carbon π-band in a crystal. However, instead of becoming a metal, the extra electron induces a pairing of the two molecules, at least at reasonably low temperatures. As a result a $C_{59}N$ dimer is formed. Only in the gas phase, at temperatures higher than 500 °C, monomers are retained with the unpaired electron.[34]

The substitution of one carbon by nitrogen on the fullerene cage introduces a dramatic symmetry breaking. Only one mirror plane is retained and the point group changes from I_h to C_s. On dimerization, some symmetry elements are regained but the overall symmetry remains as low as C_{2v}. This means all highly degenerate H_g modes from C_{60} split into nondegenerate modes. This has indeed been observed for the Raman spectra of $(C_{59}N)_2$.[35] An example is depicted in Fig. 5, spectrum (1) and (2).

The strongest line is still the pentagonal pinch mode located at 1462 cm^{-1}. For red laser excitation the radial

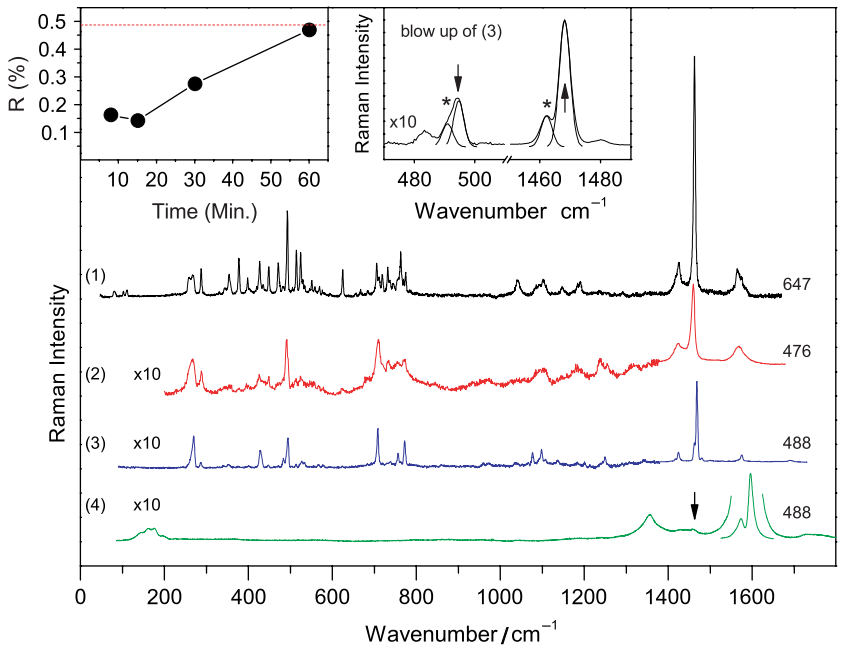

Figure 5. Raman spectra of $(C_{59}N)_2$ at 80 K excited with a red (1) and a blue (2) laser as indicated. Spectrum (3) is the response from a 1 : 1 mixture of C_{60} and $(C_{59}N)_2$ as measured in a KBr pellet. Arrows and asterisks (shown in the right inset which depicts a selected and blown up part of (3)) assign the identified lines originating from C_{60} and $(C_{59}N)_2$, respectively. The spectrum at the bottom (4) is for SWCNTs after filling with a $C_{59}N/C_{60}$ mixture. The left inset depicts the ratios R of scattering intensities between pentagonal pinch mode of encaged C_{60}, $I_{Ag(2)}$, and the intensity of the G-line of the tubes, I_G, as a function of time. The dashed line represents 90% filling. This figure is available in colour online at www.interscience.wiley.com/journal/jrs.

DOI: 10.1002/jrs

vibrations below 500 cm^{-1} appear as a striking set of peaks which can be assigned as derived from the two five-fold degenerate C_{60} modes $H_g(1)$ and $H_g(2)$ observed in C_{60} at 240 and 420 cm^{-1}, respectively. The overall scattering intensity of the spectrum is rather high but still noticeably weaker as compared to the spectra of C_{60}. To demonstrate this and for an evaluation of the filled SWCNTs to be discussed below, we have also measured a 1 : 1 mixture between C_{60} and $C_{59}N$ in a KBr pellet. The result, as plotted in Fig. 5 spectrum (3), demonstrates the dominance of the response from the C_{60} fullerene. Since the response from $C_{59}N$ is much weaker and split up into many lines on the one hand, and C_{60} has also a reasonably large number of weak Raman lines if the molecule is accommodated in a crystal[36] on the other, identification of all lines is not simple. The totally symmetric modes $A_g(1)$ and $A_g(2)$ ($A_1(1)$ and $A_1(2)$ in $(C_{59}N)_2$) are an exception. The Raman lines for these modes can be identified and are seen in Fig. 5 at 495 and 1469 cm^{-1} for the C_{60} molecule and at 492 and 1463 cm^{-1} for the $(C_{59}N)_2$ molecule, respectively. A blown up version of the corresponding part of the spectrum is depicted in the right inset of the figure. Line decomposition is indicated. The relative intensities between the response from the $C_{59}N$ molecule and the C_{60} molecule are 0.3 and 0.2 for the $A_g(1)$ and for the $A_g(2)$, respectively.

For the filling of the tubes with $(C_{59}N)_2$, it was intended to get a response from a $C_{59}N$ monomer. This cage is interesting since it carries a spin. It was attractive to get such spin-carrying molecules aligned in the nanotubes. The $(C_{59}N)_2$ dimer is known to break apart in the gas phase. This means that from the gas phase monomeric $C_{59}N$ molecules can be obtained.[34] Alternatively, it was demonstrated recently that a specially functionalized spin-neutral $C_{59}N$ molecule could be filled into the tubes from solution.[37] When the functional group was split off by heating after the molecule was filled into the tube, a magnetic molecule was retained.[38] However, it remained unclear what happened to the functional group. In our case no functional group is needed, but here as well as in the case of the filling with the $C_{59}N$ derivative it is necessary to encage spacer molecules simultaneously with the spin-carrying $C_{59}N$. This spacer molecules are expected to prevent a recombination of the $C_{59}N$ to $(C_{59}N)_2$ after it was filled into the tubes. The spectrum at the bottom of Fig. 5 depicts the Raman response for 488 nm excitation after 30 min filling from a 1:1 $C_{59}N/C_{60}$ mixture in a sealed quartz tube. The insert allows the estimation of which fraction of the two cage molecules were inserted into the tubes even after the short time of exposure. As a result, after 30 min, about 50% of the tubes which are accessible for the fullerenes are filled. Interestingly, the Raman response in the spectral range of the radial modes does not show any characteristic structures, neither from the C_{60} nor from the $C_{59}N$. In the wavenumber range of the tangential modes between 1400 and 1500 cm^{-1}, a broad but structured contribution (arrow) appears as a contribution from the filled in molecules. The signal is superimposed on the much stronger response from the D-line and the G-line of the nanotubes.

Figure 6(a) is a blow-up of the spectra from the two systems for the wavenumber range between 1400 and 1500 cm^{-1}. The intensity of the signal from the two encapsulated cages is comparable, but the signal from the C_{60} fullerene appears as a sharp line whereas the signal from the hetero-fullerene consists of a line and a broad but structured shoulder which eventually merges into the small line from the tubes. More details can be seen after subtraction of the response from the tubes (G-line and D-line). The result is depicted in part (b) of the figure. The remaining

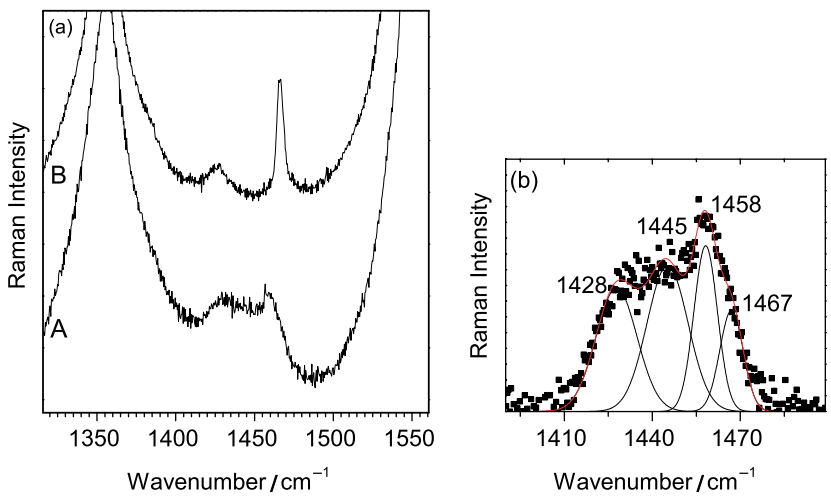

Figure 6. (a) Blow-up version of the Raman spectra for C_{60} filled (top) and $C_{59}N/C_{60}$ filled tubes (bottom). The two spectra are normalized to the response of the G-line. Part (b) depicts the response from the $C_{59}N/C_{60}$ mixture inside the tubes after subtraction of the D-line and the G-line. Smooth curves are from a line shape analysis. This figure is available in colour online at www.interscience.wiley.com/journal/jrs.

DOI: 10.1002/jrs

response can be disentangled into four main lines peaking at 1467, 1458, 1445, and 1428 cm^{-1}. The assignment of the first peak and the last peak is straightforward as originating from the encapsulated C_{60} and from the unidentified small tube line as already discussed above. The weak response from the encapsulated C_{60} is surprising but may be a consequence of the short filling time and from a partial reaction of C_{60} with $C_{59}N$ to make a hetero-dimer. The Raman response between 1467 and 1425 cm^{-1} comes from the $C_{59}N$ compounds. Their possible origin will be discussed below.

FILLING THE TUBES WITH ANTHRACENE

Anthracene ($C_{14}H_{10}$) is another interesting molecule for filling experiments. The three fused benzene rings resemble parts of the nanotube or fullerene structure but the molecule is completely flat. Its melting point is at 217 °C and it evaporates at 341 °C. Molecule stability is reported for temperatures as high as 720 °C.[39] Optical absorption starts at 3.4 eV.[39] The point symmetry of the molecule is D_{2h} and the 66 vibrational degrees of freedom are distributed as

$$\begin{aligned}\Gamma^{3N-6} = {} & 11A_g(R) + 4B_{1g}(R) + 6B_{2g} + 11B_{3g} \\ & + 6A_u + 11B_{1u}(IR) + 11B_{2u}(IR) \\ & + 6B_{3u}(IR) \end{aligned} \quad (3)$$

In the crystalline phase we expect three rotational and three translational external modes in addition to the internal modes. According to the high value for the optical transition energy, no significant resonance behavior is expected. Figure 7 depicts Raman spectra of anthracene powder as excited with various lasers and as calculated with the Gaussian03 package.

The lack of resonance is evident from the spectra for almost all laser excitations. Therefore it is not surprising that the calculated spectra give excellent agreement with the observed pattern. The only noticeable discrepancy between calculation and experiment appears between 710 and 720 cm^{-1}. Here the experiment exhibits a sharp and strong line whereas the calculation shows a distinct group of rather strong lines. The origin of this discrepancy is not clear at the moment but it may be related to the fact that the calculation was done for a molecule whereas the measurement was for the crystalline phase. The spectra are dominated by three strong lines located at 385, 752 and 1400 cm^{-1}. The normal coordinates for these lines are dominated by an extension of the molecule along its long axis, by the stretching of the central C–C bonds combined with a considerable C–H bending, and by a C═C double bond stretching motion of the atoms, respectively. In addition to the strong lines from the internal vibrations, two strong and broad lines are observed at 120 and 70 cm^{-1}, which obviously originate from the external modes. The hydrogen stretching modes have various components between 3000 and 3100 cm^{-1}. The calculated wavenumbers are scaled by a factor 0.98. The discrepancy between the observed and calculated wavenumbers in the region of the hydrogen stretching modes is less than 2%, which is within the expected accuracy of the Gaussian03 program.

In the filling experiments with anthracene, always a tube material with opened caps and with closed caps was exposed simultaneously to the anthracene environment. This allowed the control of whether the filling was really into the opened tubes as discussed above. Raman spectra after the filling process are depicted in Fig. 8.

Comparing the spectra for the exposed tubes with the opened ends to those from the pristine tubes or to the spectra from the tubes with the closed ends yields the following significant differences:

1. Several new lines appear after exposure, with the most significant ones at 1440 and 650 cm^{-1} (arrows in the figure). Several smaller lines are observable at 1397, 1260, and between 300 and 400 cm^{-1}.

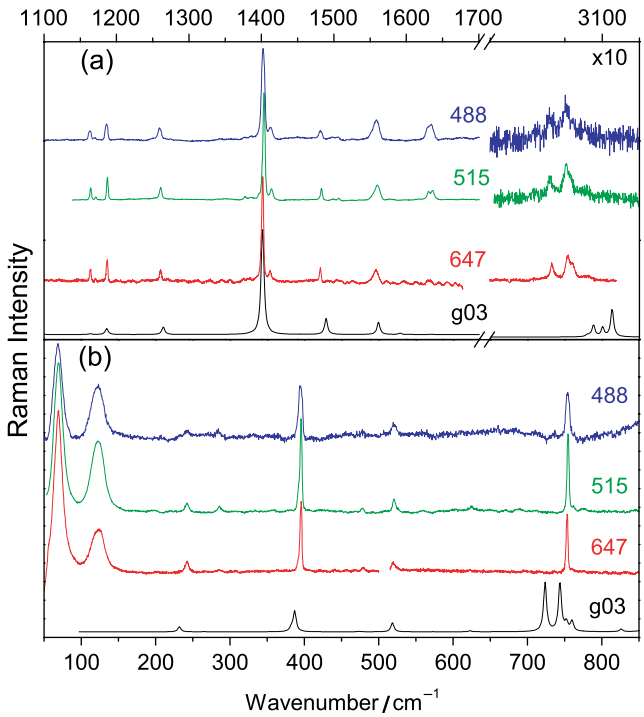

Figure 7. Room temperature Raman spectrum of anthracene as excited with three different laser lines. (a): spectra from 1100 to 1700 cm^{-1} and the spectral range of the hydrogen stretching modes. (b): low wavenumber lines. The spectra at the bottom in (a) and (b) are calculated with Gaussian03. This figure is available in colour online at www.interscience.wiley.com/journal/jrs.

DOI: 10.1002/jrs

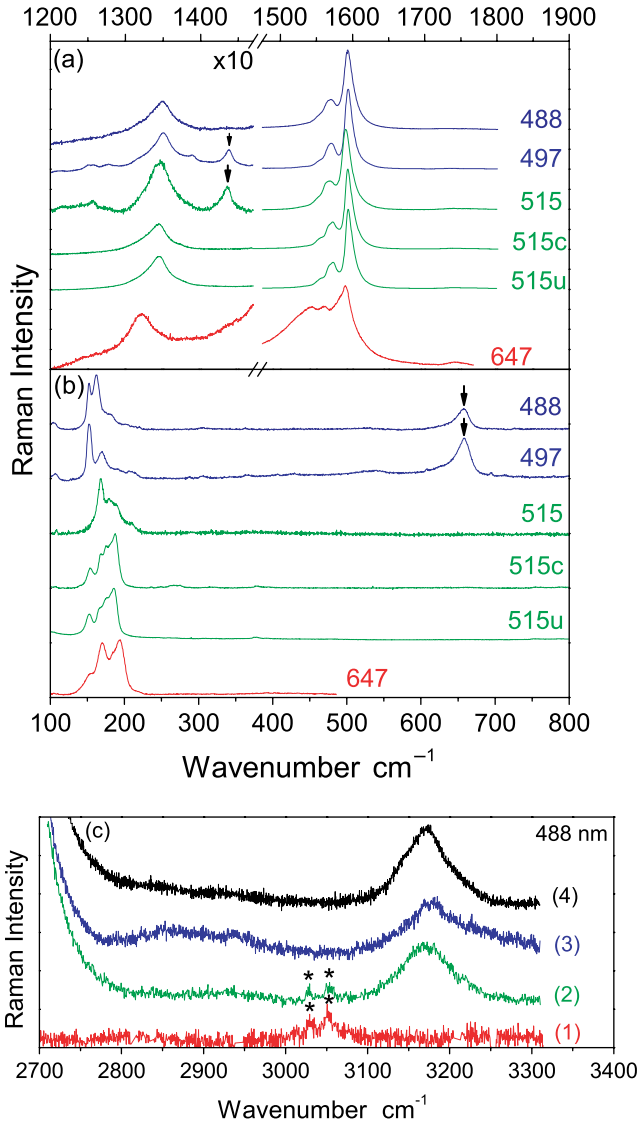

Figure 8. Raman spectra of SWCNTs after filling procedure in an anthracene environment. Spectra assigned with 'c' and 'u' in (a) and (b) are for tubes that were closed prior to exposure and for untreated tubes, respectively. Arrows indicate the modes appearing after the filling with anthracene. Part (c): hydrogen stretching modes: (1) for anthracene, (2) for a mechanical mixture between anthracene and nanotubes, (3) for opened and exposed nanotubes and (4) for pristine nanotubes. Asterisks in (c) assign the hydrogen stretching modes. This figure is available in colour online at www.interscience.wiley.com/journal/jrs.

2. The intensities of the new modes exhibit some dependence on the laser energy. For example, the new mode at 1440 cm^{-1} is not observed with the deep blue and with the red laser.
3. In the spectral range between 3000 and 3100 cm^{-1} the response from the hydrogen stretching mode has almost disappeared. The strong broad peak at 3200 cm^{-1} in spectra (2) to (4) represents the overtone of the G-line. On the low wavenumber end of the spectra (2) to (4) the signal approaches the response from the D2 line.
4. The response from the RBM of the tubes has significantly changed its pattern. Whereas for the pristine tube material the strongest component of the RBM is at the high wavenumber edge of the pattern, it appears at the low wavenumber edge for the anthracene filled tubes. This effect is particularly strong for green laser excitation.

All these new features are not observed for the co-exposed sample as demonstrated in the spectrum labeled as 515c. This spectrum appears almost unchanged as compared to the spectrum from the untreated material, labeled as 515u in the figure.

DISCUSSION

The closing procedure demonstrated in the 'Experimental Procedure' section is a very reliable check on the success of the filling process. The tube ends need not really to be closed. It is enough that the orifice at the tube ends becomes small enough such that fullerenes or other large molecules like anthracene cannot enter any more. The very small concentration of inner tubes that is observed even in the case of the closed tubes may come from some carbon impurities which are always around in the tube material. It has been observed frequently even in the case of high-temperature annealing of opened but otherwise untreated tubes.

For the assignment of the response observed from the encapsulated $C_{59}N$ molecule, three species have to be considered: the $C_{59}N$ monomer, the $C_{59}N$ dimer and the $C_{59}N/C_{60}$ hetero-dimer. According to the low temperature of the experiment, most of the $C_{59}N$ molecules will condense into either a dimer or a hetero-dimer. Only a few geometrically isolated species may stay as a monomer. Therefore, it is suggestive to assign the peak at 1458 cm^{-1} to the $C_{59}N$ dimer and the broad response just below it to the Raman signal from the hetero-dimer. Since part of the low wavenumber part of the signal is rather broad, contributions from $C_{59}N$ degradation products cannot be excluded.

With respect to the Raman response described for the spectra of the anthracene-exposed tubes, it can be concluded that the anthracene molecules have entered the the tubes. The surprising result is the significant change of the Raman spectra of the molecule after filling. The experience from filling tubes with fullerenes or with other molecules suggests that only rather small changes in the spectra are to be expected. In the case of anthracene the changes are dramatic. The strongest anthracene mode is upshifted by 40 cm^{-1}, the other strong anthracene line is downshifted by almost 100 cm^{-1} and the anthracene line close to 400 cm^{-1} and the hydrogen stretching modes almost disappeared. One possibility to understand these results may be traced back

to a substantial change of the molecular structure after encapsulation. The anthracene may have clustered into a larger compound elongated along the tube axis and thus lost some hydrogen. The clustering would also reduce the HOMO-LUMO gap, which provides the possibility for resonance enhancement in the visible.

The strong change of the RBM of the tubes is unusual. From experience with other fillers, only minor changes in the line pattern were expected. The strong modification of the RBM response may be related to the strong change of the response from the anthracene itself. This effect is diameter-selective. The small-diameter tubes suffer from a much stronger decrease in intensity as compared to the large-diameter tubes. This is not unreasonable since the interaction with the fillers can be expected to be stronger for these tubes. A possibility for the decrease of Raman intensity is an enhanced charge transfer from the inside to the enclosing tubes, thus changing the resonances of the latter.

CONCLUSIONS

From the experiments performed, it is concluded that Raman scattering is an excellent method to study the process of filling SWCNTs with various molecules. The opening of the tubes before the filling process is crucial. On the one hand, it can be done reversibly with respect to a temperature-induced closing of the tubes. The use of unopened tubes in a filling experiment allows, on the other hand, checking the success of the filling process. This is done by critically comparing the spectra obtained from opened and closed tubes.

In the case of filling the tubes with the hetero-fullerene $C_{59}N$, filling from the gas phase is demonstrated. Since $C_{59}N$ is unstable at high temperatures, short filling times are recommended. Even though spacer molecules such as C_{60} were used, the compounds eventually existing inside the tubes are $(C_{59}N)_2$ dimers or hetero-dimers. The response from individual C_{60} molecules is almost completely lost.

Anthracene is a challenging material for filling the SWCNTs. As far as its size is concerned, it should fit easily into the tubes. From the experiments performed, we conclude that filling was successful but the molecule experiences a considerable modification. Our results suggest that hydrogen is lost and the Raman cross-section becomes sensitive to the energy of the exciting laser.

Acknowledgments

This work was supported by the Fonds zur Förderung der Wissenschaftlichen Forschung in Österreich, project 17345 and by the ESF-EUROCORES project IMPRESS (FWF project I83-N20), and conducted as part of the award ('Functionalization of Carbon Nanotubes Encapsulating Novel Carbon-based Nanostructured Materials') made under the European Heads of Research councils and European Science Foundation EURYI (European Young Investigator) Award scheme, by funds from the Participating Organizations of EURYI and EC Sixth Framework Programme. F.S. acknowledges support from the Hungarian State Grants No. TS049881, F61733 and NK60984.

REFERENCES

1. Smith BW, Monthioux M, Luzzi DE. *Nature* 1998; **396**: 323.
2. Sloan J, Kirkland AI, Hutchison JL, Green MLH. *Chem. Commun.* 2002; 1319.
3. Hulman M, Kuzmany H, Costa PMFJ, Friedrichs S, Green MLH. *Appl. Phys. Lett.* 2004; **85**: 2068.
4. Sloan J, Carter R, Meyer RR, Vlandas A, Kirkland AI, Lindan PJD, Lin G, Harding J, Hutchison JL. *Phys. Status Solidi B* 2006; **243**: 3257.
5. Yanagi K, Miyata Y, Kataura H. *Adv. Mater.* 2006; **18**: 437.
6. Maniwa Y, Kataura H, Abe M, Suzuki S, Achiba Y, Kira H, Matsuda K. *J. Phys. Soc. Jpn.* 2002; **71**: 2863.
7. Jorio A, Souza Filho AG, Dresselhaus G, Dresselhaus MS, Saito R, Hafner JH, Lieber CM, Matinaga FM, Dantas MSS, Pimenta MA. *Phys. Rev. B* 2001; **63**: 245416.
8. Kuzmany H, Pfeiffer R, Kramberger C, Pichler T, Liu X, Knupfer M, Fink J, Kataura H, Achiba Y, Smith BW, Luzzi DE. *Appl. Phys. A* 2003; **76**: 449.
9. Saito R, Dresselhaus G, Dresselhaus MS. *Physical Properties of Carbon Nanotubes*. Imperial College Press: London, 1998.
10. Reich S, Thomsen C, Maultzsch J. *Carbon Nanotubes. Basic Concepts and Physical Properties*. Wiley-VCH: Weinheim, 2004.
11. Rao AM, Richter E, Bandow S, Chase B, Eklund PC, Williams KA, Fang S, Subbaswamy KR, Menon M, Thess A, Smalley RE, Dresselhaus G, Dresselhaus MS. *Science* 1997; **275**: 187.
12. Hulman M, Plank W, Kuzmany H. *Phys. Rev. B* 2001; **63**: 081406.
13. Dresslehaus MS, Dresselhaus G, Inomata D, Nakao D, Saito R. *Mol. Mater.* 1994; **4**: 27.
14. Dobardžić E, Milošević I, Nikolić B, Vuković T, Damnjanović M. *Phys. Rev. B* 2003; **68**: 045408.
15. Barros EB, Jorio A, Samsonidze GG, Capaz RB, Souza Filho AG, Filho JM, Dresselhaus G, Dresselhaus MS. *Phys. Rep.* 2006; **431**: 261.
16. Saito R Kataura H. Optical properties and Raman spectroscopy of carbon nanotubes. In *Carbon Nanotubes. Synthesis, Structure, Properties, and Applications*, *Volume 80 of Topics in Applied Physics*, Dresselhaus MS, Dresselhaus G, Avouris P (eds). Springer: Berlin, Heidelberg, 2001; 213.
17. Fantini C, Jorio A, Souza M, Strano MS, Dresselhaus MS, Pimenta MA. *Phys. Rev. Lett.* 2004; **93**: 147406.
18. Bachilo SM, Strano MS, Kittrell C, Hauge RH, Smalley RE, Weisman RB. *Science* 2002; **298**: 2361.
19. Kramberger C, Pfeiffer R, Kuzmany H, Zólyomi V, Kürti J. *Phys. Rev. B* 2003; **68**: 235404.
20. Telg H, Maultzsch J, Reich S, Hennrich F, Thomsen C. *Phys. Rev. Lett.* 2004; **93**: 177401.
21. Amer MS, El-Ashry MM, Maguire JF. *J. Chem. Phys.* 2004; **121**: 2752.
22. Meyer JC, Paillet M, Michel T, Moréac A, Neumann A, Duesberg GS, Roth S, Sauvajol J-L. *Phys. Rev. Lett.* 2005; **95**: 217401.
23. Kürti J, Zólyomi V, Grüneis A, Kuzmany H. *Phys. Rev. B* 2002; **65**: 165433.
24. Dubay O, Kresse G, Kuzmany H. *Phys. Rev. Lett.* 2002; **88**: 235506.
25. Popov VN, Lambin P. *Phys. Rev. B* 2006; **73**: 165425.
26. Wang F, Dukovic G, Brus LE, Heinz TF. *Science* 2005; **308**: 838.
27. Ando T. *J. Phys. Soc. Jpn.* 1997; **66**: 1066.
28. Kataura H, Maniwa Y, Kodama T, Kikuchi K, Hirahara K, Suenaga K, Iijima S, Suzuki S, Achiba Y, Krätschmer W. *Synth. Met.* 2001; **121**: 1195.

29. Hasi F, Simon F, Kuzmany H. *J. Nanosci. Nanotech.* 2005; **5**: 1785.
30. Bandow S, Takizawa M, Hirahara K, Yudasaka M, Iijima S. *Chem. Phys. Lett.* 2001; **337**: 48.
31. Pfeiffer R, Simon F, Kuzmany H, Popov VN. *Phys. Rev. B* 2005; **72**: 161404(R).
32. Simon F, Kukovecz A, Kramberger C, Pfeiffer R, Hasi F, Kuzmany H. *Phys. Rev. B* 2005; **71**: 165439.
33. Simon F, Kuzmany H, Rauf H, Pichler T, Bernardi J, Peterlik H, Korecz L, Fülöp F, Janossy A. *Chem. Phys. Lett.* 2004; **383**: 362.
34. Simon F, Arcon D, Tagmatarchis N, Garaj S, Forro L, Prassides K. *J. Phys. Chem. A* 1999; **103**: 6969.
35. Kuzmany H, Plank W, Winter J, Dubay ONT, Prassides K. *Phys. Rev. B* 1999; **60**: 1005.
36. Matus M, Kuzmany H. *Appl. Phys. A* 1993; **56**: 241.
37. Simon F, Kuzmany H, Bernardi J, Hauke F, Hirsch A. *Carbon* 2006b; **44**: 1958.
38. Simon F, Kuzmany H, Nafradi B, Feher T, Forro L, Janossy A, Rockenbauer A, Korecz L, Hauke F, Hirsch A. *Phys. Rev. Lett.* 2006a; **97**: 136801.
39. Ferguson J, Reeves L, Schneider W. *Can. J. Chem.* 1957; **35**: 1117.

DOI: 10.1002/jrs